

Measuring the ionization balance of gold in EBIT
plasmas of importance to ICF

Mark J. May

B-Division

Lawrence Livermore National Laboratory



Experiment

P. Beiersdorfer
M. Schneider
S. Terracol
K. Wong
G. Brown

Modeling

S. Hansen
H.K. Chung
M. Gu (Stanford)
K. Fournier
B. Wilson
J. Scofield
K. Reed

GSFC-NASA

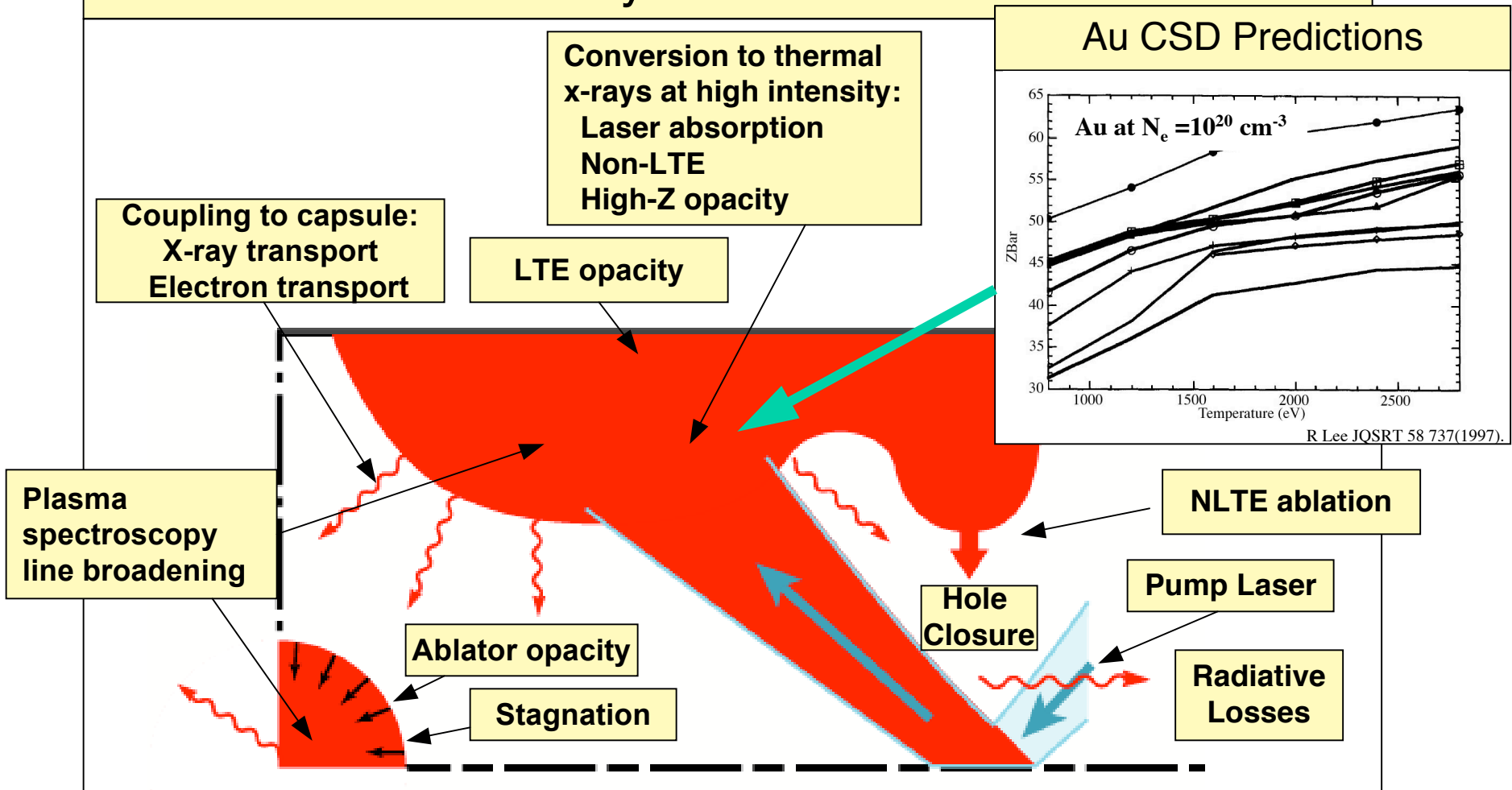
F.S. Porter
R. Kelley
C. Kilbourne
K. Boyce

20 Years of Spectroscopy with the Electron Beam Ion Trap
November 12 - 16, 2006 Berkeley, California

Accurate models for non-LTE physics are necessary for ICF

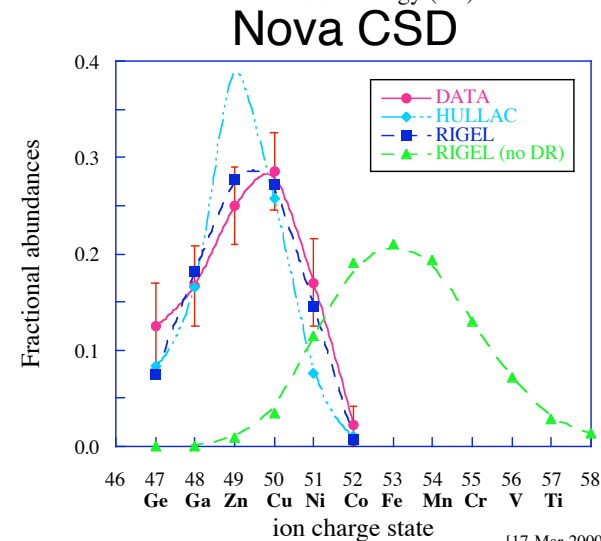
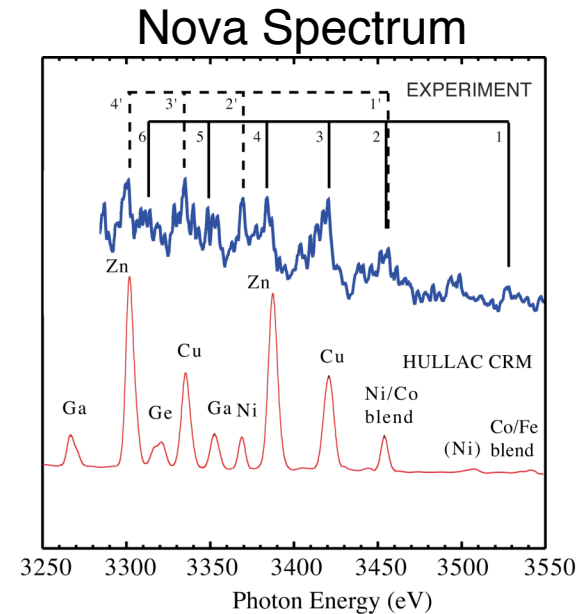
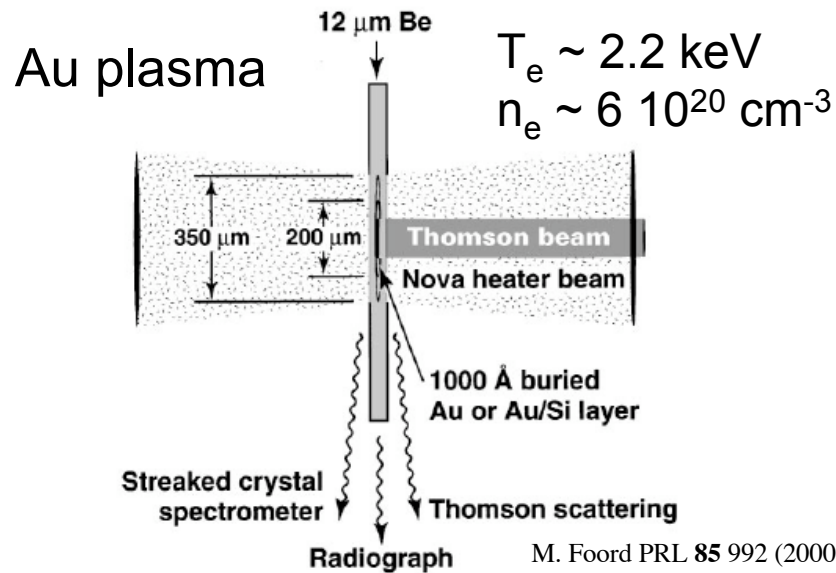


Atomic Physics Needs for ICF



Experiments are required to improve theoretical models

Previous charge balance measurements from NOVA distinguish between models at high density

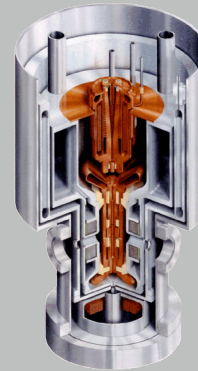
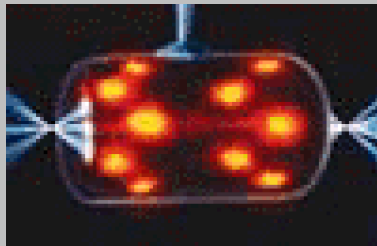


- CSD by fitting detailed HULLAC computations to the measured line emission
 - EA/DR corrections / Optical depth corrections
- Analysis of the complex spectrum is challenging in the high density plasma
 - Many competing atomic physics processes
 - Spatial gradients
 - Transient nature of the experiment
 - Differences between HULLAC and experimental photon energies

Au Charge State Distribution Experiments



Omega and Helen Electron Beam Ion Trap Lasers



T_e (keV)	5 - 10	2 - 3
E_{Beam} (keV)	-	2.5 - 6.5
N_e (cm ⁻³)	3×10^{21}	1×10^{12}

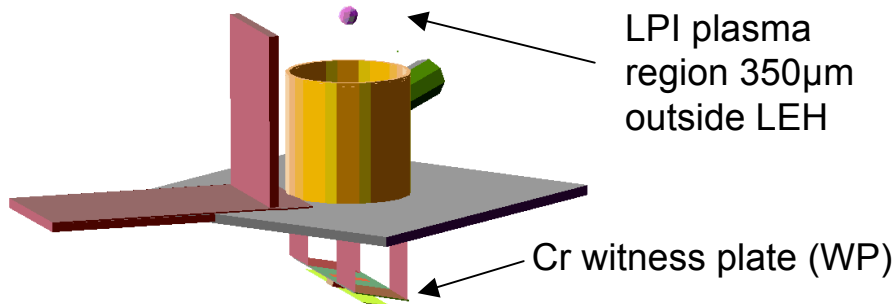
Gold Ionization States	Ni - P 51+ - 64+	Kr - Ar 43+ - 61+
Spectral Regions	M-band: 5f→3d 3 - 5.0 keV L-band: 3d→2p 8.5 - 12.5 keV	M-band: 4f→3d & 5f→3d 2 - 6 keV RR: n = 4, 5, 6, etc 6 - 8 keV
Spectrometers	Space and Time Res.	Time Resolved



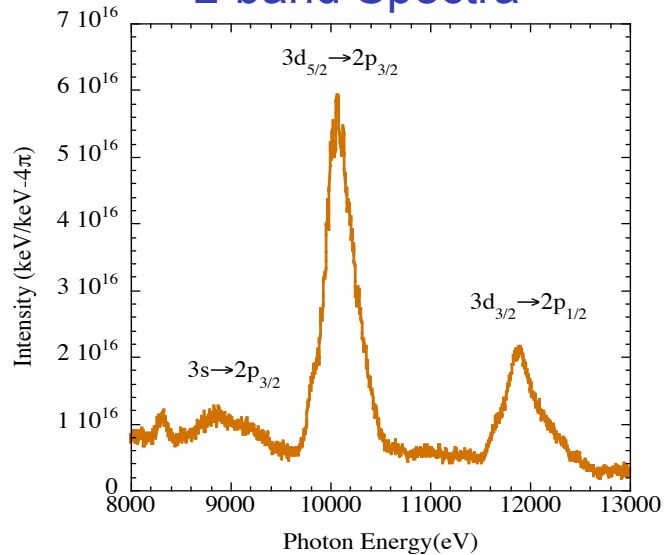
High Temperature Plasmas in Hot Halfraums at the OMEGA Laser



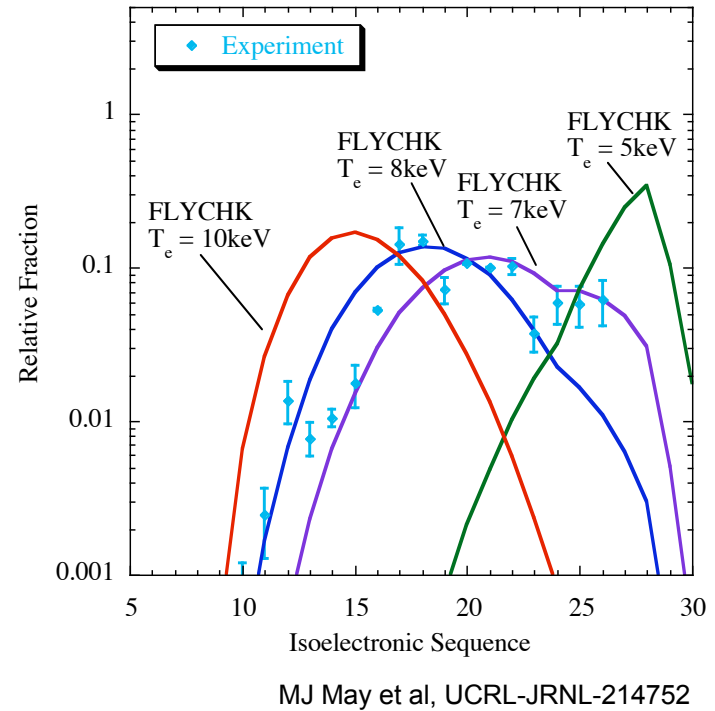
Hot Halfraum Target



L-band Spectra



Inferred Halfraum CSD



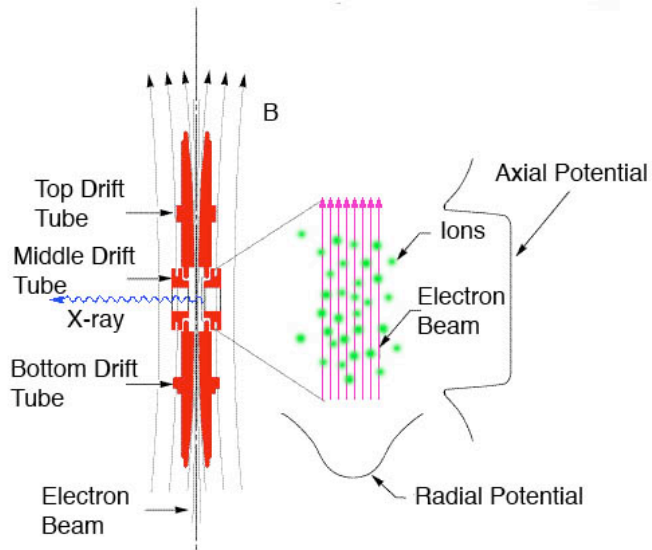
Experiments are required at even higher electron temperatures



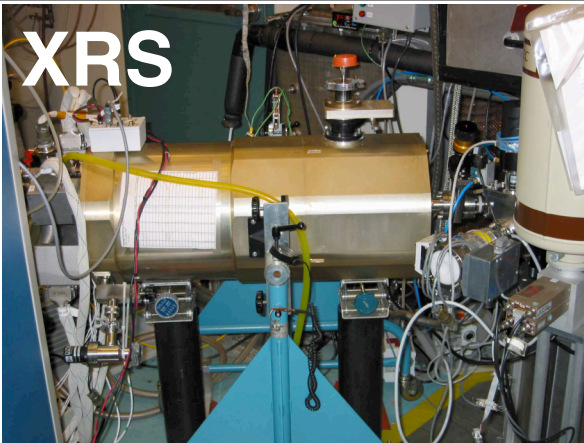
EBIT measurements test models at low density



Conceptual View EBIT-I



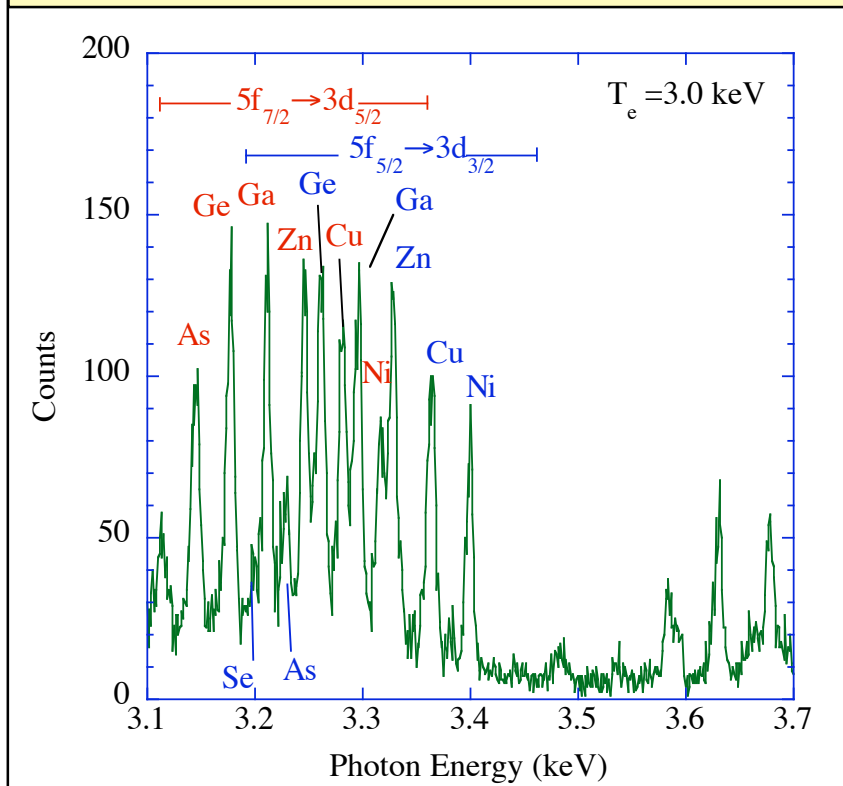
- Electron Beam Ion Trap (EBIT-I and EBIT-II)
 - Gold Plasmas
 - $E_{\text{Beam}} = 2.75, 3.0, 3.6, 4.6, 5.5, 6.0, 6.5$ keV
 - $T_e = 2.0, 2.5, 3.0$ keV
 - $n_e \sim 1 \times 10^{12} \text{ cm}^{-3}$
 - Fewer active atomic physics processes than in high density plasmas
 - Steady state plasmas
- Gold Measurements/Modeling
 - Ni-like to Kr-like Gold lines ($E_{\text{photon}} = 0.1 - 8.0$ keV)
 - Spectrometers: XRS microcalorimeter (GSFC), Crystal, Grating
 - Collisional line emission (CE) and radiative recombination (RR) measurements
 - CSD inferred from both CE and RR spectral measurements
 - Collisional excitation cross sections inferred from the CE and RR measurements



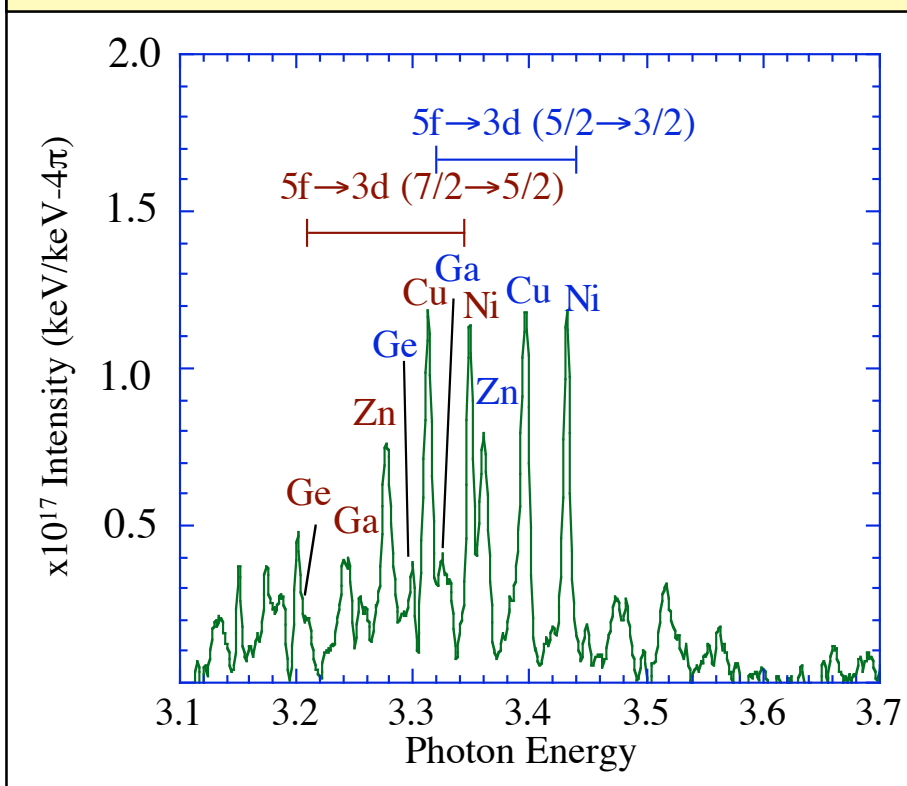
EBIT spectrum helps interpret Au foil spectrum from laser plasmas



EBIT-I XRS Spectrum



AWE Au Foil Spectrum



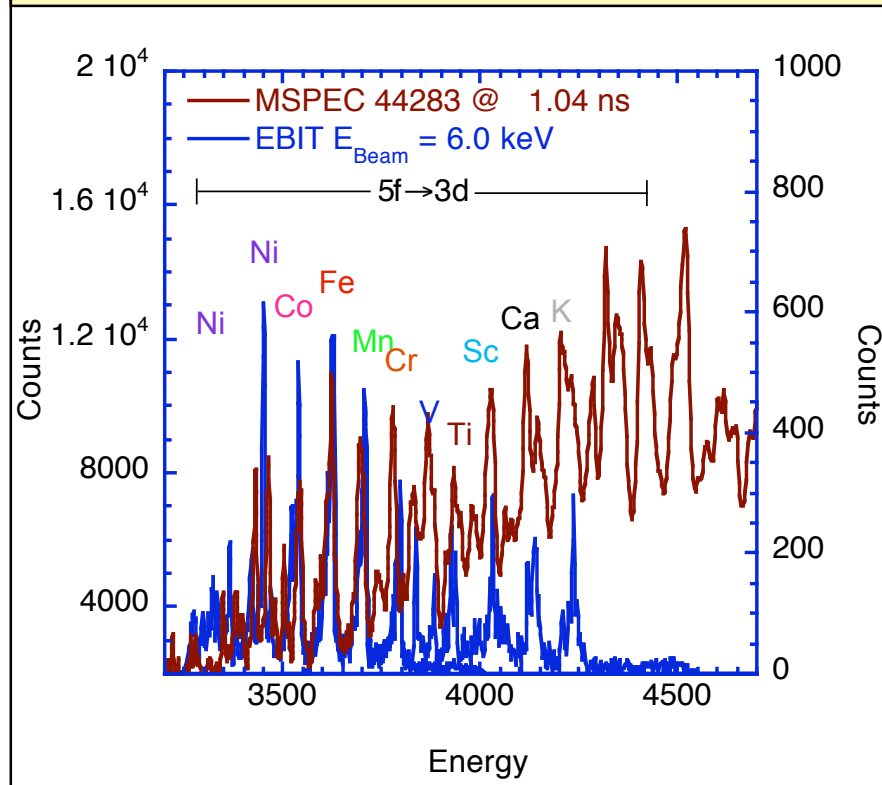
Low density spectrum allows unambiguous line identification of laser spectrum



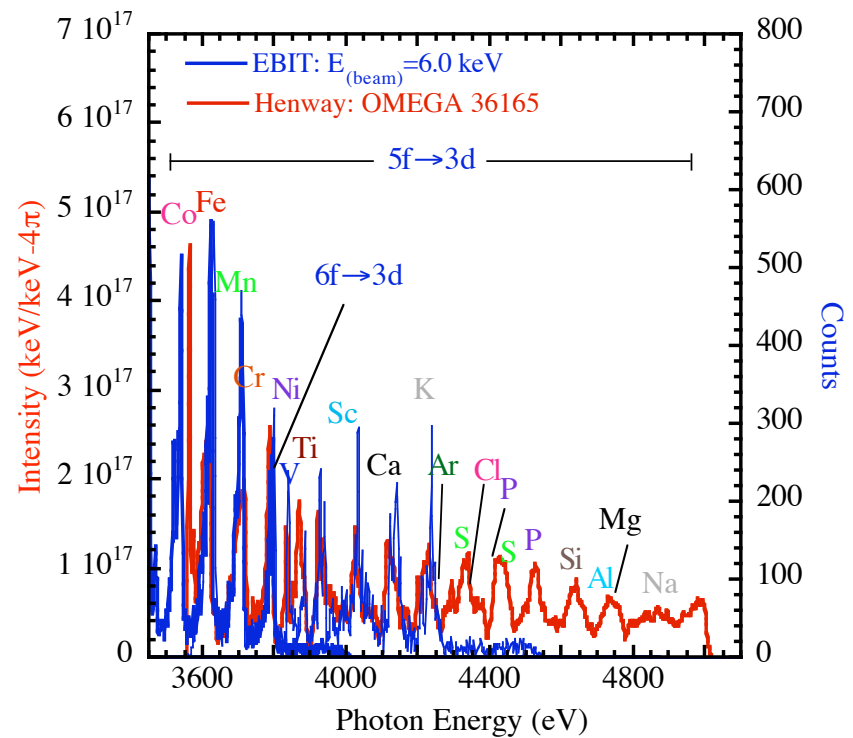
Direct Comparisons of EBIT and OMEGA Spectra



EBIT and MSPEC Spectra



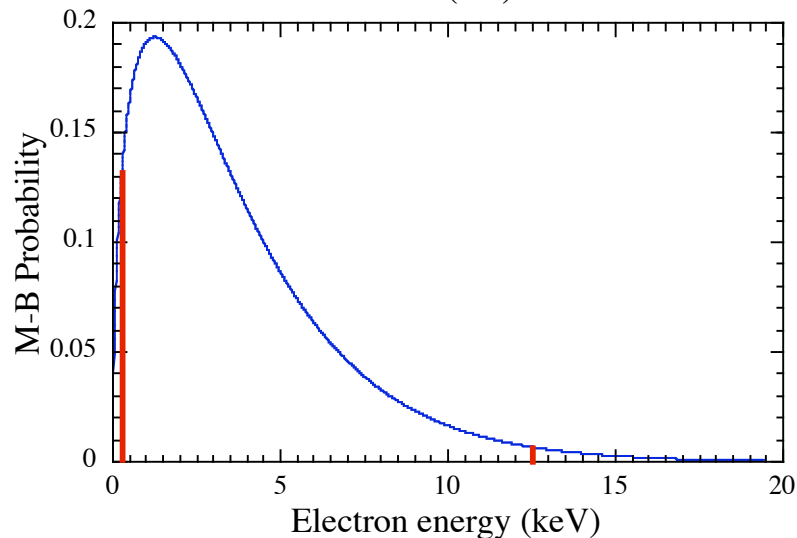
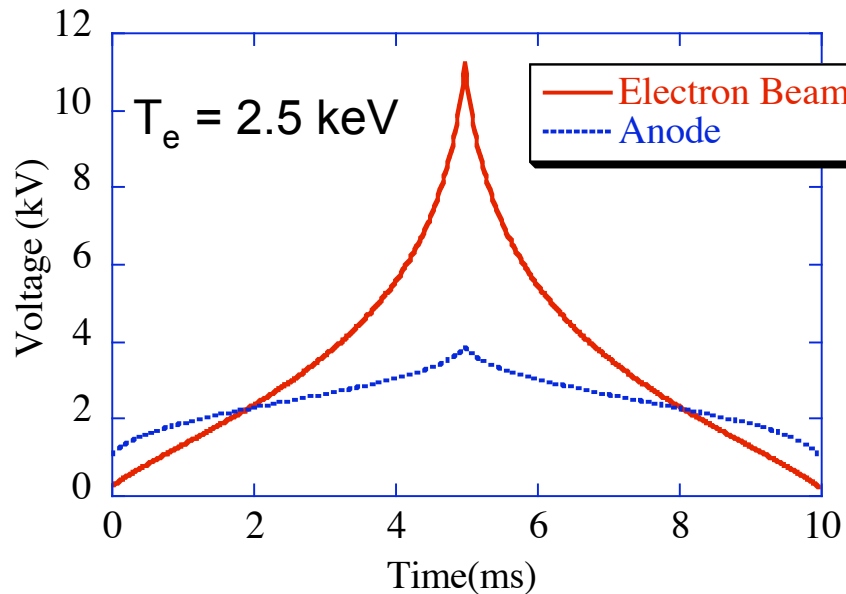
EBIT and Henway Spectra



EBIT spectra useful in identification and energy calibration of OMEGA spectra



LLNL EBIT produces simulated Maxwell-Boltzmann plasmas

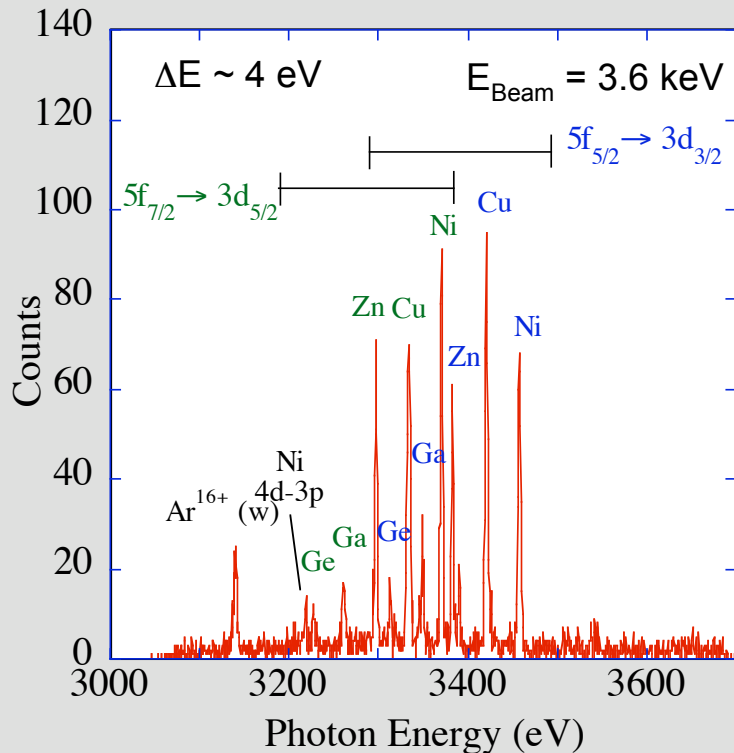


- Simulated a Maxwell-Boltzmann (MB) electron distribution
- Monoenergetic electron beam is swept in time by an arbitrary waveform generator
- Time spent at one beam energy is proportional to the MB distribution at that energy
- Anode Voltage (V_A) swept to maintain constant n_e in beam
- Sample a large fraction of the MB distribution
- Sweep time $\sim 5 \text{ ms}$.

Complementary X-ray measurements provide two approaches to measure the CSD in EBIT

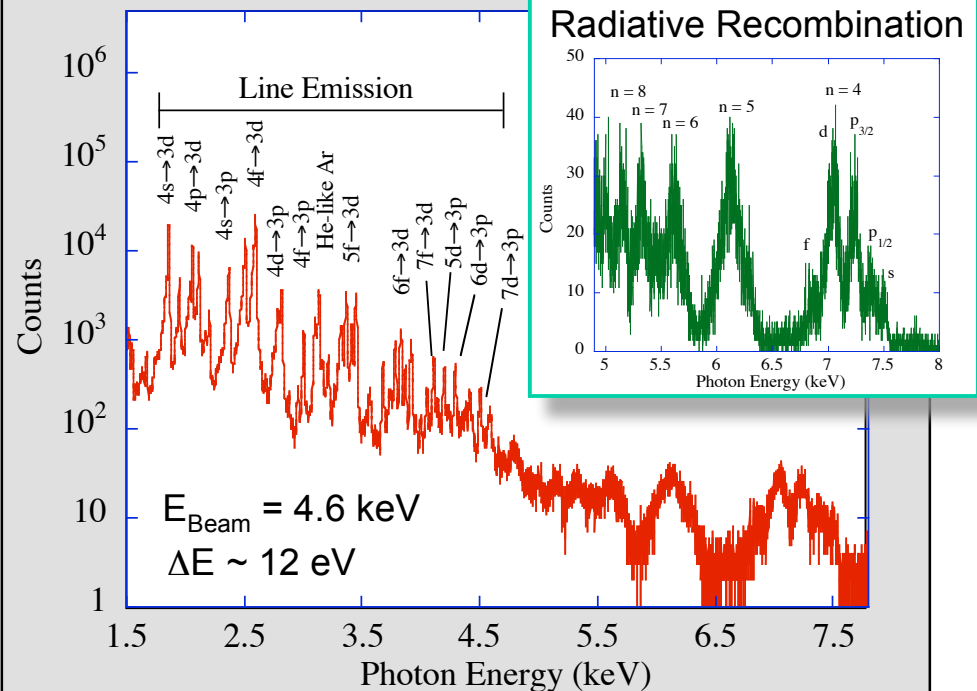


Crystal Spectrum



- High resolution allows line spectra to be used to infer charge balance (NOVA approach)

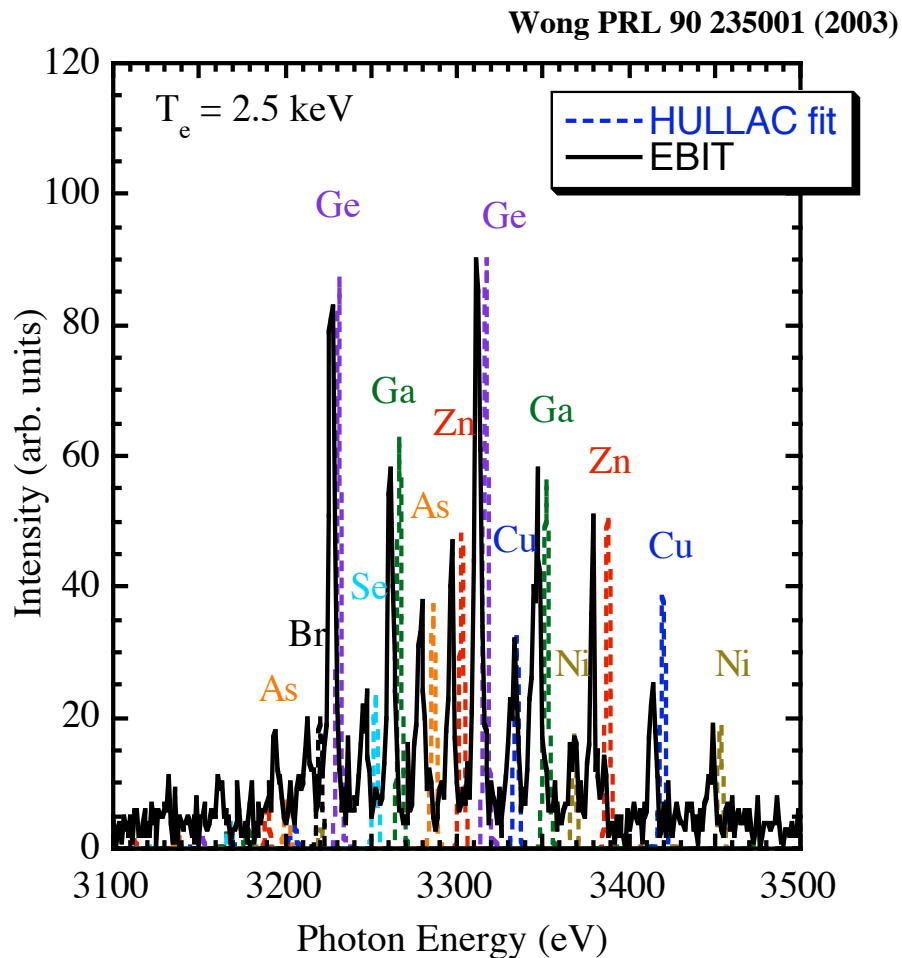
XRS Spectrum



- Broadband spectra used to infer charge balance from RR peaks
- Technique is independent of line excitation models



Gold CSD from EBIT inferred from X-ray spectra and fit with HULLAC calculations

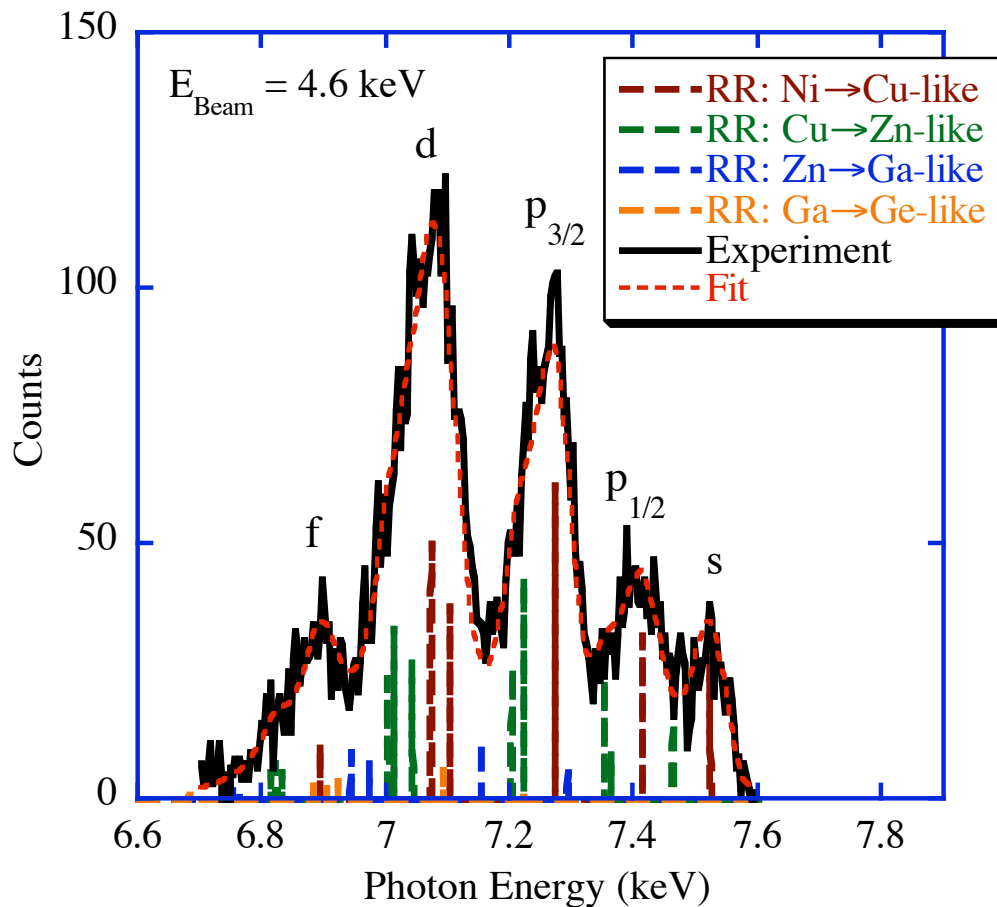


- Crystal spectrometer: $5f \rightarrow 3d$ and $4f \rightarrow 3d$ transitions
- Each HULLAC charge state is coupled to the higher charge state to include the effects of DR on line intensities
- CSD is inferred by individually fitting each HULLAC charge state model to the measurement

Accurate CSD inferred from the line emission spectra



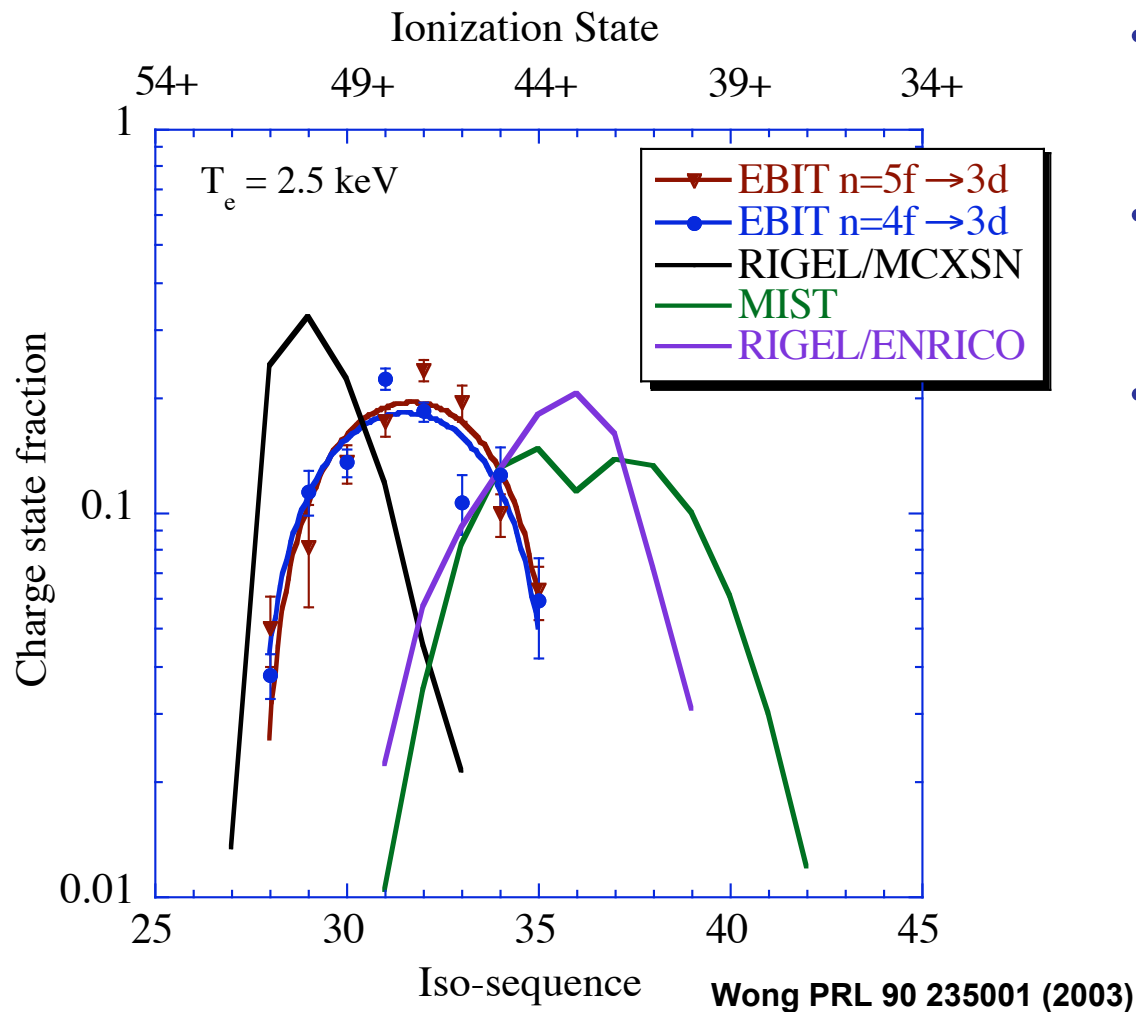
Radiative recombination spectrum from EBIT and fit with GRASP RR calculations



- XRS microcalorimeter: Radiative Recombination (RR) spectrum
- Beam Plasma
- $\Delta E_{\text{Beam}} \sim 70 \text{ eV}$
- CSD is inferred by fitting the RR spectrum with accurate Grasp calculations (Scofield)

Accurate CSD independent of the line emission spectra

Gold CSD from EBIT thermal plasmas compared to simulations



- EBIT: Inferred from the $n=5f \rightarrow 3d, 4f \rightarrow 3d$ spectra
- MCXSN/ENRICO: high density code
- MIST: tokamak transport code: low density

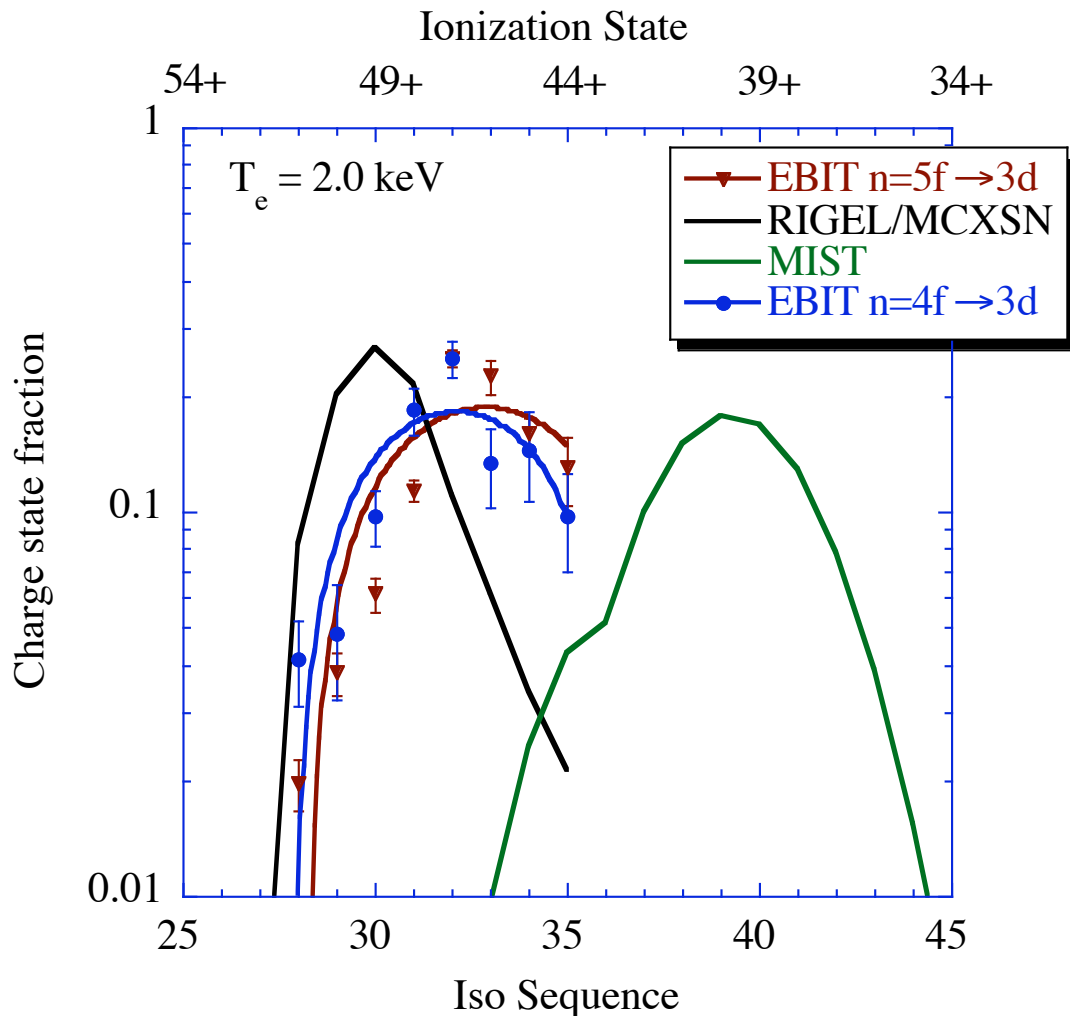
Z_{eff} Results

EBIT ($5f \rightarrow 3d$)	46.8 ± 0.8
EBIT ($4f \rightarrow 3d$)	47.5 ± 0.3
ENRICO	43.7
MCXSN	49.5
MIST	42.7

Significant discrepancy between experiment and simulation



Gold CSD from EBIT thermal plasmas compared to simulations



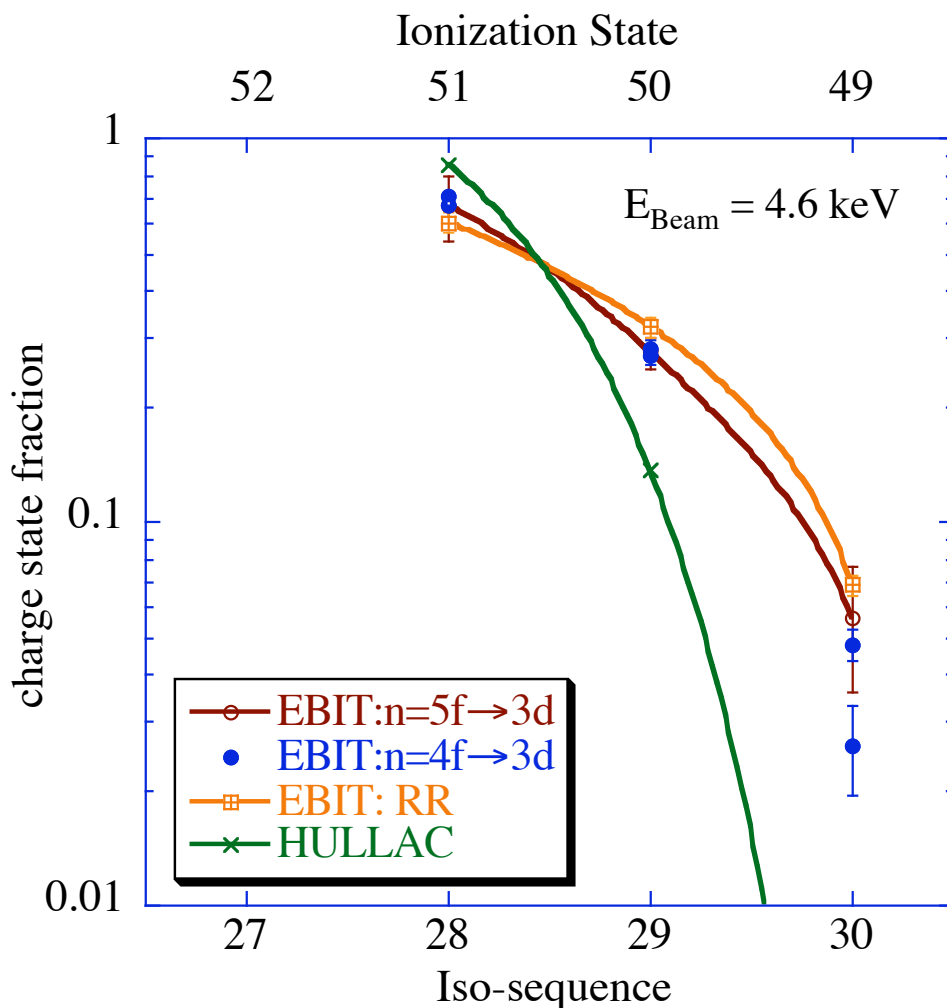
- EBIT: Inferred from the $n=5f \rightarrow 3d$ and $4f \rightarrow 3d$ spectra
- MCXSN: high density code
- MIST: tokamak transport code: low density

Z_{eff} Results

EBIT ($5f \rightarrow 3d$)	46.5 ± 0.9
EBIT ($4f \rightarrow 3d$)	46.9 ± 0.5
MCXSN	48.5
MIST	39.9

Significant discrepancy between experiment and simulation at other temperatures

Gold CSD from EBIT beam plasmas compared to simulations

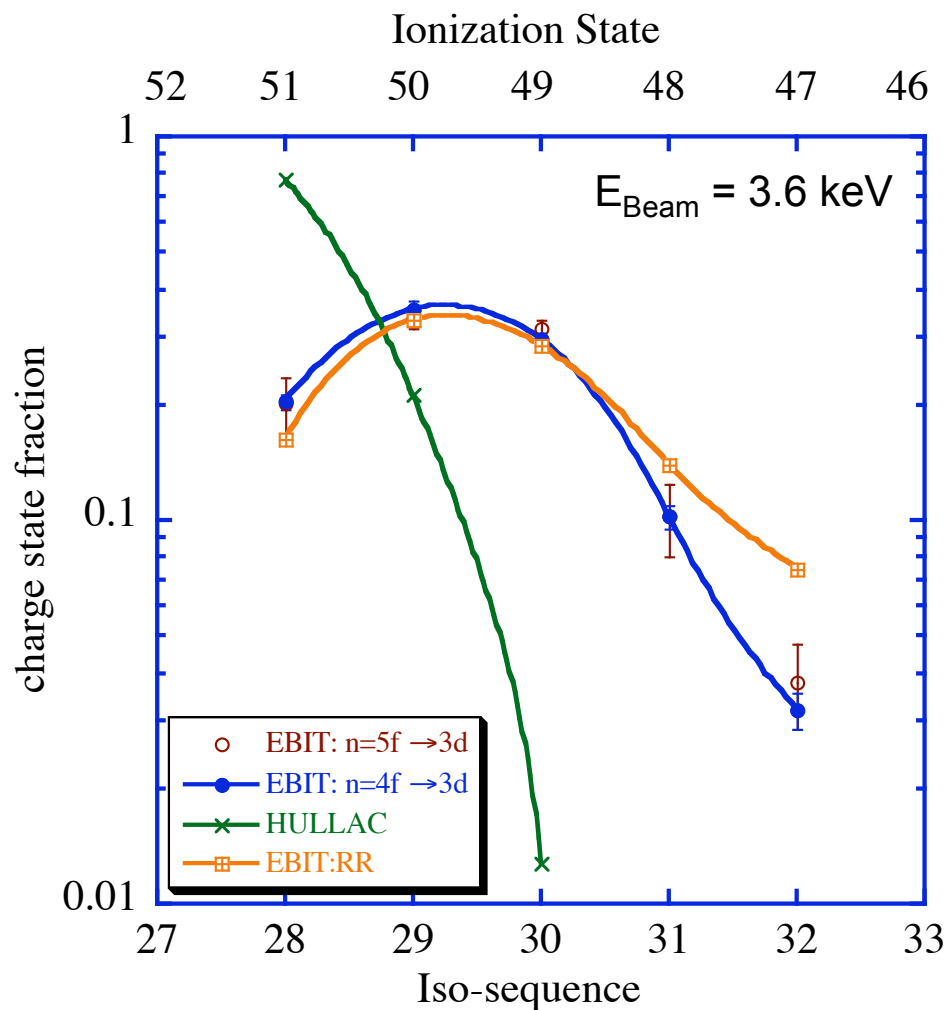


- EBIT: Inferred from both the $n = 5f \rightarrow 3d$ and $4f \rightarrow 3d$ spectra and the RR spectrum
- HULLAC: modeling CSD
- I_p (Ni-like) ~ 4.9 keV

Z_{eff} Results	
EBIT (5f \rightarrow 3d)	50.7 ± 1.4
EBIT (4f \rightarrow 3d)	50.5 ± 1.0
EBIT (RR)	50.5 ± 1.0
HULLAC	50.9

Experimental results are self-consistent but disagree with HULLAC

Gold CSD from EBIT beam plasmas compared to simulations



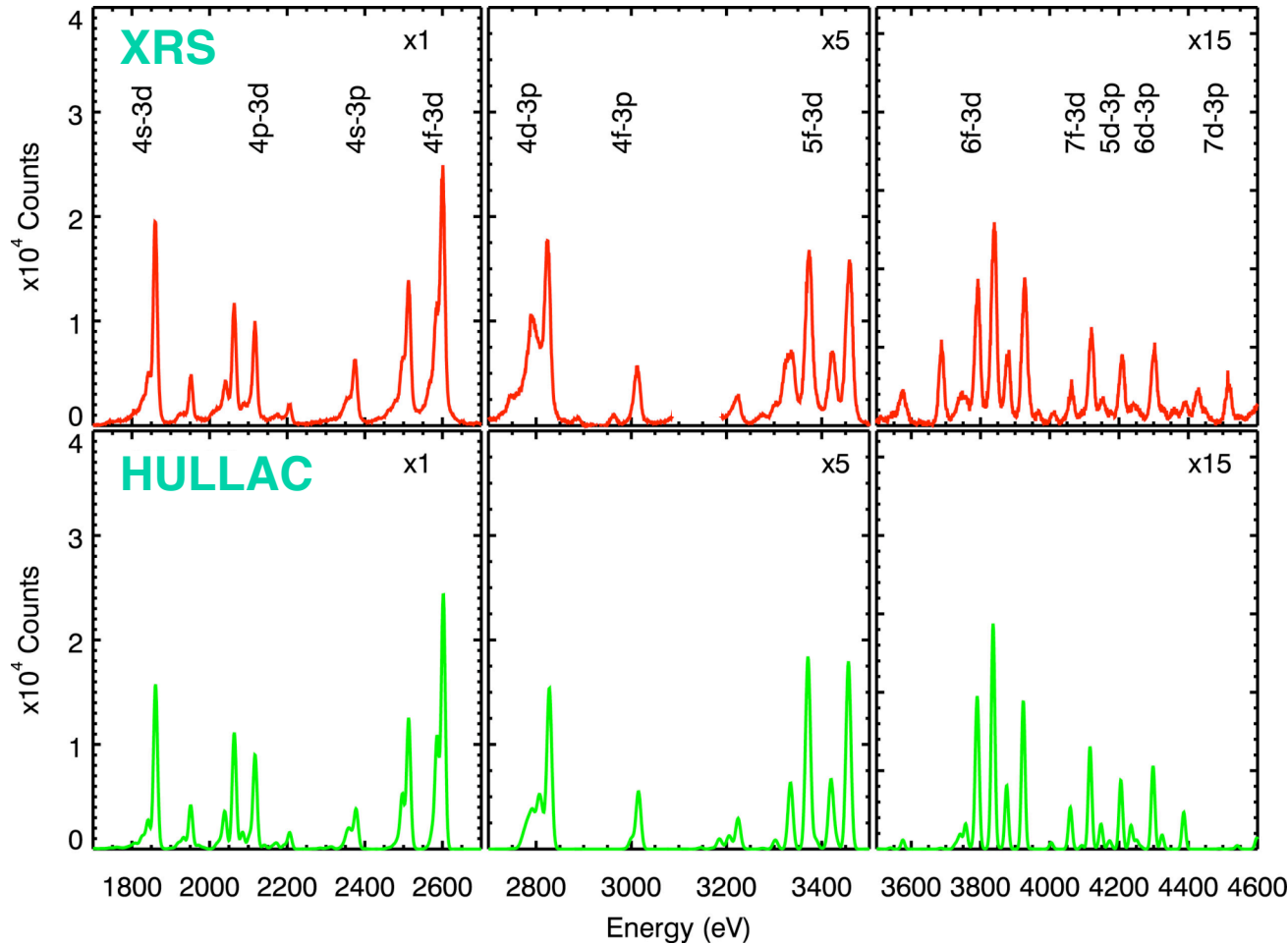
- EBIT: Inferred from both the $n = 5f \rightarrow 3d$ and $4f \rightarrow 3d$ spectra and the RR spectrum
- HULLAC: modeling CSD

Z_{eff} Results	
EBIT ($5f \rightarrow 3d$)	49.8 ± 1.2
EBIT ($4f \rightarrow 3d$)	49.8 ± 0.8
EBIT:RR	49.4 ± 0.3
HULLAC	50.8

Experimental results are self-consistent but disagree with HULLAC at other beam energies



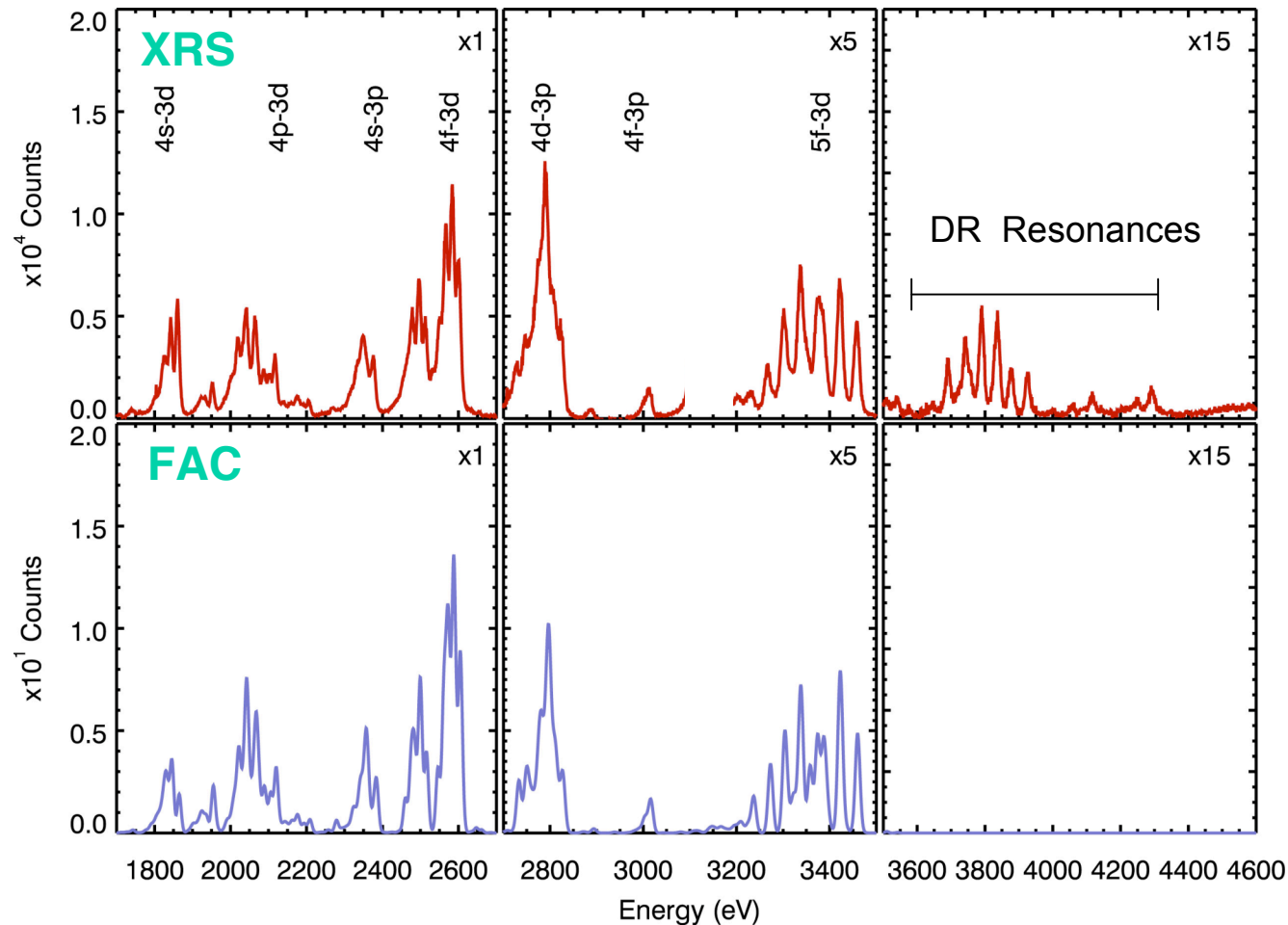
Modeling of XRS Microcalorimeter Spectrum from EBIT with HULLAC



- $E_{\text{Beam}} = 4.6 \text{ keV}$
- XRS microcalorimeter Spectrum
 - Photometrically Calibrated
 - 1.5 - 5 keV
- HULLAC Modeling
 - Ni,Cu,Zn-like
 - $n=4 \rightarrow 4$, $n=4 \rightarrow 3$ to $7 \rightarrow 3$
 - Use experimentally Inferred CSD

HULLAC modeling reproduces collisionally excited microcalorimeter spectrum

Modeling of XRS Microcalorimeter Spectrum from EBIT with FAC



- $E_{\text{Beam}} = 3.6 \text{ keV}$
- XRS Spectrum
 - Photometrically Calibrated
 - 1.5 to 5 keV
- FAC Modeling
 - Ni,Cu,Zn,Ga,Ge-like
 - $n=4 \rightarrow 4$, $n=4 \rightarrow 3$ to $5 \rightarrow 3$
 - Experimentally Inferred CSD

FAC modeling reproduces collisionally excited XRS spectrum at other beam energies



XRS microcalorimeter spectra can be used to infer collisional excitation cross sections



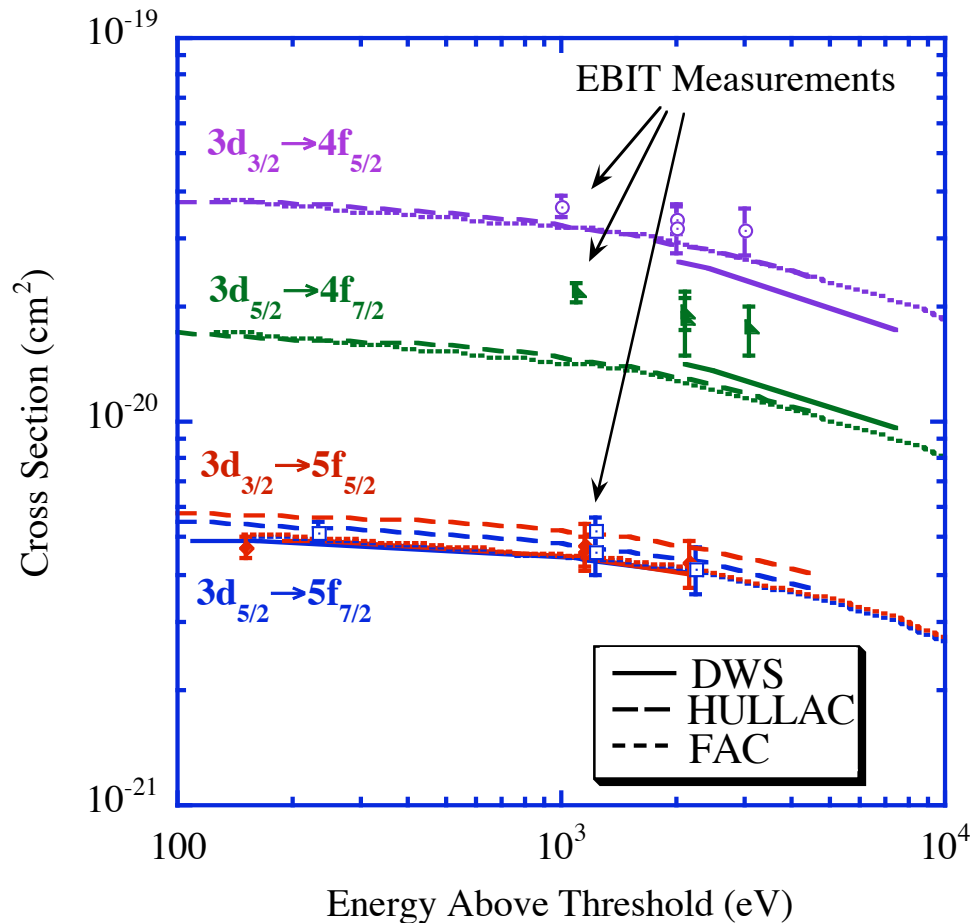
- Verify the electron impact collisional excitation cross sections, σ^{CE} , from HULLAC utilized in the CSD analysis
- Measured the σ^{CE} from the XRS CE line and RR emissions

$$\sigma^{\text{CE}} = \frac{\sum_j G_j^{\text{RR}} \eta_j^{\text{RR}} T_j^{\text{RR}} \sigma_j^{\text{RR}}}{G^{\text{CE}} \eta^{\text{CE}} T^{\text{CE}}} \frac{I^{\text{CE}}}{I^{\text{RR}}}$$

- I - intensities, σ - cross section, η - detector efficiency, T - filter transmissions
- G -angular distribution of the polarization, P
 - Dipole Transition $G = 3/(3-P)$
- Polarization of the line emission from the EBIT Plasma
 - Magnetic sub-level cross sections provided by K. Reed
 - Ni-like $5f_{5/2} \rightarrow 3d_{3/2}$ ($J=1 \rightarrow 0$)
 - $P = (\sigma_{-1} - 2\sigma_0 + \sigma_{+1}) / (\sigma_{-1} + 2\sigma_0 + \sigma_{+1})$
 - $P \sim 0.3$; $G \sim 0.91$ at $E_{\text{Beam}} = 4.6$ keV



Measured and theoretical collisional impact cross sections: Ni-like Gold

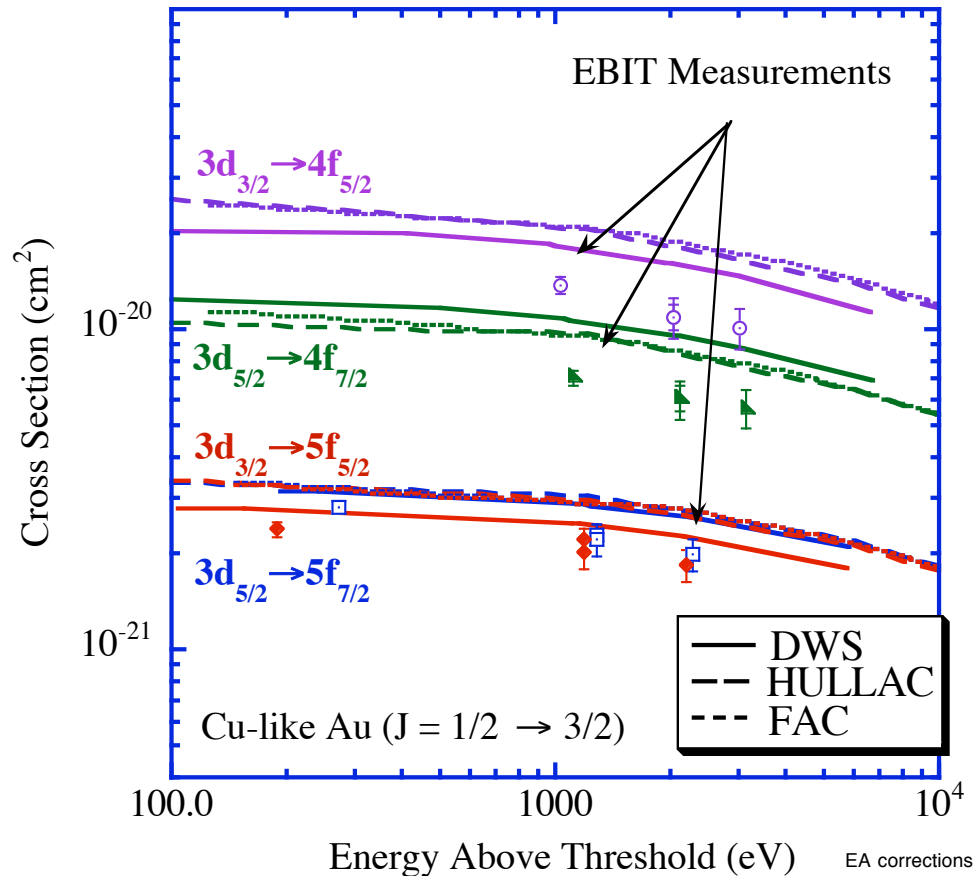


- EBIT: Measured direct impact collisional excitation rates
 - Ni-like Au
 - $n = 3d \rightarrow 5f, 3d \rightarrow 4f$
- Theory:
 - HULLAC
 - K. Reed
 - FAC
- $3d \rightarrow 5f$:
 - Reasonable Agreement
- $3d \rightarrow 4f$:
 - Measurement ~ 1.5 times theory

Measurements demonstrate errors in some excitation rates



Measured and theoretical collisional impact cross sections: Cu-like Gold



- EBIT: Direct impact collisional excitation rates
 - Cu-like Au
 - $n = 3d \rightarrow 5f, 3d \rightarrow 4f$
- Theory:
 - HULLAC
 - DWS (K. Reed)
 - FAC
- $3d \rightarrow 5f$
 - Reasonable Agreement
 - EA Corrections
 - $B(5/2 \rightarrow 3/2) = 0.832$
 - $B(7/2 \rightarrow 5/2) = 0.800$
- $3d \rightarrow 4f$:
 - Exp. ~ 0.7 of theory

Errors are larger for some Cu-like cross sections

Conclusions



- CSD Determinations
 - Beam plasmas: CE line emission and RR
 - Simulated thermal plasmas: CE line emission
 - Discrepancies with calculations
- Successfully modeled the EBIT-I beam plasma XRS microcalorimeter spectra
- Measured the collisional excitation cross sections
 - Ni-, Cu- and Zn-like gold $n=3d \rightarrow 4f$ and $3d \rightarrow 5f$
 - Some Discrepancies with theory
 - Extend this to Ga - Kr-like Au